

Mutant Vasopressin Precursors That Cause Autosomal Dominant Neurohypophyseal Diabetes Insipidus Retain Dimerization and Impair the Secretion of Wild-type Proteins*

(Received for publication, September 2, 1998, and in revised form, January 12, 1999)

Mika Ito, Richard N. Yu, J. Larry Jameson[‡], and Masafumi Ito

From the Division of Endocrinology, Metabolism, and Molecular Medicine, Northwestern University Medical School, Chicago, Illinois 60611

Autosomal dominant familial neurohypophyseal diabetes insipidus is caused by mutations in the arginine vasopressin (AVP) gene. We demonstrated recently that mutant AVP precursors accumulate within the endoplasmic reticulum of neuronal cells, leading to cellular toxicity. In this study, the possibility that mutant AVP precursors interact with wild-type (WT) proteins to alter their processing and function was explored. WT and mutant precursors were epitope-tagged to allow them to be distinguished in transfected cells. An *in vivo* cross-linking reaction revealed homo- and heterodimer formation between WT and mutant precursors. Mutant precursors were also shown to impair intracellular trafficking of WT precursors from the endoplasmic reticulum to the Golgi apparatus. In addition to the cytotoxicity caused by mutant AVP precursors, the interaction between the WT and mutant precursors suggests that a dominant-negative mechanism may also contribute to the pathogenesis of familial neurohypophyseal diabetes insipidus.

Familial neurohypophyseal diabetes insipidus (FNDI)¹ (1) is caused by a deficiency of arginine vasopressin (AVP), a hormone that controls serum osmolality by altering renal free water clearance (1). Diabetes insipidus is transmitted as an autosomal dominant trait in these families. A large number of distinct mutations have been found in the AVP gene (2–15).

The AVP gene encodes polypeptide precursors consisting of a signal peptide, AVP, neurophysin (NP), and glycoprotein domains (16). Prepro-AVP is synthesized in the magnocellular neurons of the hypothalamus and is converted to pro-AVP by the removal of the signal peptide. Pro-AVP undergoes several post-translational processing steps, including the addition of carbohydrate side chains and proteolytic cleavage to yield AVP, NP, and the glycoprotein. These products are stored within neurosecretory vesicles in the axonal terminals of the posterior pituitary gland and are secreted into the blood in response to osmotic stimuli (17).

Most of the mutations in individuals with FNDI have been

found within the signal peptide and the NP domains (18). A substitution of Thr for Ala at the carboxyl terminus of the signal peptide (A(–1)T) is the most commonly found mutation, and it has been identified in various ethnic groups, suggesting independent mutational events. Mutations within the NP domain include amino acid substitutions, a single amino acid deletion, and premature protein termination. Despite the presence of a normal allele, FNDI patients develop diabetes insipidus, although the symptoms are not usually manifest until several months or years after birth. These features have raised questions concerning the molecular pathogenesis of the disorder. A limited number of autopsy studies have demonstrated a paucity of AVP-producing neurons in the hypothalamus of patients with FNDI (19–22). Consistent with these pathologic findings, magnetic resonance imaging has revealed an absence of the bright spot that characterizes the posterior pituitary gland in a subset of patients with FNDI (12). Based on these observations, it has been postulated that mutant AVP precursors might be cytotoxic to AVP-producing neurons.

In a previous study (4), the A(–1)T mutation was shown to cause inefficient cleavage of the signal peptide, giving rise to aberrant precursors that were glycosylated, but not cleaved, by signal peptidase. This finding raised the possibility that the aberrant precursors might accumulate and lead to cellular toxicity. In support of this idea, the expression of several different FNDI mutants was shown to impair the intracellular trafficking of mutant AVP precursors and the viability of neuroblastoma cells (23).

The cytotoxicity of mutant AVP precursors may be sufficient to account for the autosomal dominant mode of inheritance of FNDI. However, in some autosomal dominant diseases, the mutant protein exerts dominant-negative activity to alter the function of the normal allele (24). AVP precursors have been shown to physically interact with each other *in vitro* (25). It is therefore possible that mutant AVP precursors could form heterodimers with wild-type (WT) protein products to alter their function and contribute to the pathogenesis of FNDI. In this study, we examined the physical and functional interactions between WT and mutant AVP precursors by expressing epitope-tagged precursors in cultured cells.

EXPERIMENTAL PROCEDURES

Plasmid Constructions—Expression vectors for the WT and mutant (G57S (2), A(–1)T (4), ΔE47 (5), and C67X (9)) AVP precursors (Fig. 1A) have been described previously (23). For epitope tagging (Fig. 1B), restriction sites for *Cla*I, *Spe*I, and *Xba*I (ATCGAT ACTAGT TCTAGA) were introduced by polymerase chain reaction immediately after the last codon of the glycoprotein domain (WT, G57S, A(–1)T, and ΔE47) or the 66th codon of the NP domain (C67X), and the resulting vectors were digested with *Cla*I and *Xba*I. Annealed oligonucleotides containing the Myc-His tag or the influenza hemagglutinin (HA) tag, along with sequence overhangs for the *Cla*I and *Xba*I sites, were ligated into the same restriction sites in the plasmid vectors (Fig. 1B). The Myc-His tag

* The costs of publication of this article were defrayed in part by the payment of page charges. This article must therefore be hereby marked "advertisement" in accordance with 18 U.S.C. Section 1734 solely to indicate this fact.

[‡] To whom correspondence should be addressed: Div. of Endocrinology, Metabolism, and Molecular Medicine, Northwestern University Medical School, Tarry 15-709, 303 E. Chicago Ave., Chicago, IL 60611. Tel.: 312-503-0469; Fax: 312-503-0474; E-mail: lameson@nwu.edu.

¹ The abbreviations used are: FNDI, familial neurohypophyseal diabetes insipidus; AVP, arginine vasopressin; NP, neurophysin; WT, wild-type; HA, hemagglutinin; BFA, brefeldin A; ER, endoplasmic reticulum; PAGE, polyacrylamide gel electrophoresis; Endo H, endoglycosidase H; DSS, disuccinimidyl suberate.

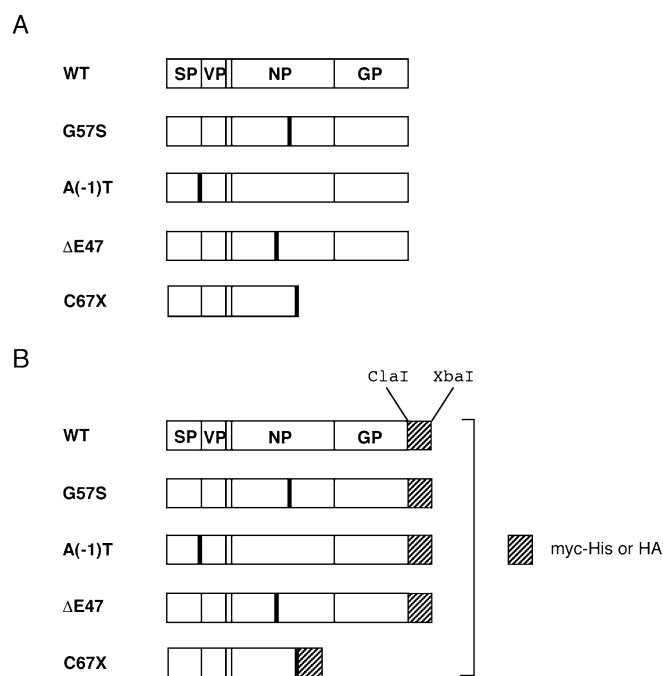


FIG. 1. Strategy for epitope tagging of the AVP precursors. *A*, the structure of the AVP precursors is shown along with the four AVP mutants analyzed in this study. Mutations include a substitution of Ser for Gly at amino acid 57 (G57S), a replacement of Ala at the carboxyl terminus of the signal peptide (position -1) with Thr (A(-1)T), a deletion of Glu at position 47 (Δ E47), and a premature termination at position 67 (C67X) in the NP domain. *SP*, signal peptide; *VP*, vasopressin; *GP*, glycoprotein. *B*, restriction sites for *Cla*I and *Xba*I were introduced immediately after the last codon of the WT and mutant AVP precursors. DNA cassettes encoding epitopes were ligated into the *Cla*I and *Xba*I sites, giving rise to expression vectors for epitope-tagged WT and mutant AVP precursors.

contains the c-Myc epitope (EQKLISEEDL), the intervening amino acid sequence (NSAVD), and polyhistidine sequence (His_6) from the pcDNA3.1MycHis expression vector (Invitrogen, San Diego, CA). The His_6 sequence is added to allow protein purification. The amino acid sequence of the HA tag is YPYDVPDYA. After polymerase chain reaction and subcloning, the entire cDNA sequence was verified by the dideoxy-mediated chain termination method (26). All the cDNAs were introduced into the pRc/RSV vector (Invitrogen). The vector without a cDNA insert was used as a control in some experiments.

Cell Culture and Transfection—Human embryonic kidney tsa 201 cells (27) were grown in Dulbecco's modified Eagle's medium supplemented with 10% fetal bovine serum in a 5% CO_2 atmosphere at 37 °C. Cells were transfected by the calcium phosphate method as described previously (28). In precursor interaction assays (see below), cells were treated with 10 $\mu\text{g}/\text{ml}$ brefeldin A (BFA) (Sigma) for 12 h to inhibit protein transport from the endoplasmic reticulum (ER) to the Golgi apparatus (29).

Metabolic Labeling and Immunoprecipitation—Continuous metabolic labeling and immunoprecipitation were performed as described previously (23). Briefly, transiently transfected cells were labeled for 12 h in Dulbecco's modified Eagle's medium containing 100 μCi of $\text{Expres}^{35}\text{S}$ protein labeling mixture (DuPont). Cell extracts and culture medium were subjected to immunoprecipitation using polyclonal anti-AVP or anti-NP antibodies (ICN, Costa Mesa, CA). Immunoprecipitates were separated by 16.5% SDS-polyacrylamide gel electrophoresis (PAGE) followed by autoradiography. For pulse-chase analyses, transfected cells were labeled for 15 min with 100 μCi of $\text{Expres}^{35}\text{S}$ protein labeling mixture in 0.5 ml of methionine- and cysteine-free Dulbecco's modified Eagle's medium and chased using 1 ml of complete Dulbecco's modified Eagle's medium containing 100 $\mu\text{g}/\text{ml}$ cycloheximide (Sigma). Cycloheximide was added to completely inhibit further synthesis of labeled precursors after the pulse labeling. In some experiments, immunoprecipitates were treated with endoglycosidase H (Endo H) (New England Biolabs Inc., Beverly, MA) according to the instructions of the manufacturer. Densitometric analyses were performed using a GS-700 imaging densitometer (Bio-Rad). Quantitative analyses were performed with film exposures in the linear range.

Precursor Interaction Assays—Cells transfected with expression vectors for precursors, with or without the Myc-His epitope tag, were labeled for 12 h in the presence of 10 $\mu\text{g}/\text{ml}$ BFA. After labeling, cells were lysed in buffer A (20 mM Tris (pH 8.0), 150 mM NaCl, 1% Triton X-100, 5 mM imidazole, 1 mM phenylmethylsulfonyl fluoride, 1 $\mu\text{g}/\text{ml}$ aprotinin, 1 $\mu\text{g}/\text{ml}$ leupeptin, and 1 $\mu\text{g}/\text{ml}$ pepstatin A). Cell extracts were incubated with the Talon metal affinity resin (CLONTECH, Palo Alto, CA) in the presence of 10 mM imidazole for 30 min at 4 °C with gentle rocking. After extensive washing in buffer A containing 15 mM imidazole, bound proteins were eluted from the resin by boiling in SDS-PAGE sample buffer containing dithiothreitol and subjected to 16.5% SDS-PAGE followed by autoradiography. For the *in vitro* precursor interaction assay, WT precursors with and without the Myc-His tag were translated *in vitro* using the TNT reticulocyte lysate system (Promega, Madison, WI) in the presence of [^{35}S]methionine (DuPont) and canine microsomal membranes (Promega). The [^{35}S]methionine-labeled proteins were subjected to the binding reaction with metal affinity resin as described above. Extensive washing and the inclusion of imidazole throughout the assay are necessary to reduce nonspecific protein interactions. Under these conditions, <10% of the total input protein is typically bound to the affinity resin (30).

In Vivo Cross-linking and Western Blot Analysis—A non-cleavable cross-linker, disuccinimidyl suberate (DSS) (Pierce), was dissolved in dimethyl sulfoxide at a concentration of 100 mM. For the detection of homodimers, cells expressing precursors with the HA tag were collected in phosphate-buffered saline and then incubated in either phosphate-buffered saline containing Me_2SO (1:100 dilution) or phosphate-buffered saline containing 1 mM DSS for 30 min at room temperature. Immediately after performing the cross-linking reaction, cells were lysed in a buffer containing 20 mM Hepes (pH 7.9), 420 mM NaCl, 20% glycerol, 1.5 mM MgCl_2 , 1 mM phenylmethylsulfonyl fluoride, 1 $\mu\text{g}/\text{ml}$ aprotinin, 1 $\mu\text{g}/\text{ml}$ leupeptin, and 1 $\mu\text{g}/\text{ml}$ pepstatin A. Whole cell extracts were subjected to 15% reducing SDS-PAGE followed by electrotransfer to polyvinylidene difluoride membranes (Boehringer Mannheim). Membranes were probed with horseradish peroxidase-conjugated anti-HA antibody (Boehringer Mannheim) according to the instructions of the manufacturer. Subsequently, proteins were detected using the enhanced chemiluminescence detection system (Boehringer Mannheim). For the detection of heterodimers as well as homodimers, cells expressing precursors with the Myc-His tag and those with the HA tag were subjected to an *in vivo* cross-linking reaction as described above. After the reaction, cells were lysed in buffer A, and cell extracts were incubated with the metal affinity resin as described above for the precursor interaction assay. Bound proteins were eluted from the resin and separated by 15% SDS-PAGE under reducing conditions. After Western blot transfer, membranes were probed with the anti-HA antibody.

RESULTS

Processing of WT AVP Precursors—Human embryonic kidney tsa 201 cells were transiently transfected with an empty vector or with expression vectors for WT AVP precursors with or without the Myc-His epitope tag to allow studies of precursor expression and processing. After continuous metabolic labeling, cell extracts and medium were harvested and subjected to immunoprecipitation. A 14-kDa protein (Fig. 2A, lanes 3, 5, 9, and 11) was detected in cells transfected with an empty vector (lanes 1 and 7), suggesting that this band is nonspecific. Using the anti-NP antibody, a similar series of precursors were identified, independent of the presence of the Myc-His epitope tag. The WT AVP precursor was 21 kDa (lane 3), whereas the intracellular precursor containing the Myc-His epitope tag was 25 kDa (lane 5). The expression levels of the 21- and 25-kDa precursors for the WT and Myc-His-tagged AVP precursors were similar. The intracellular precursors consisted of doublets (lanes 3 and 5), presumably reflecting different states of glycosylation. In the medium, the 22-kDa (WT) (lane 4) and 26-kDa (Myc-His) (lane 6) precursors as well as a 12-kDa protein were detected. The sizes of the precursors in the medium were increased relative to those in the cell extracts, reflecting the addition of carbohydrate moieties prior to secretion (Fig. 2B). Each of the precursor forms and the 12-kDa protein were also immunoprecipitated with the anti-AVP antibody (Fig. 2A, lanes 9–12), indicating that they contain both the AVP and NP

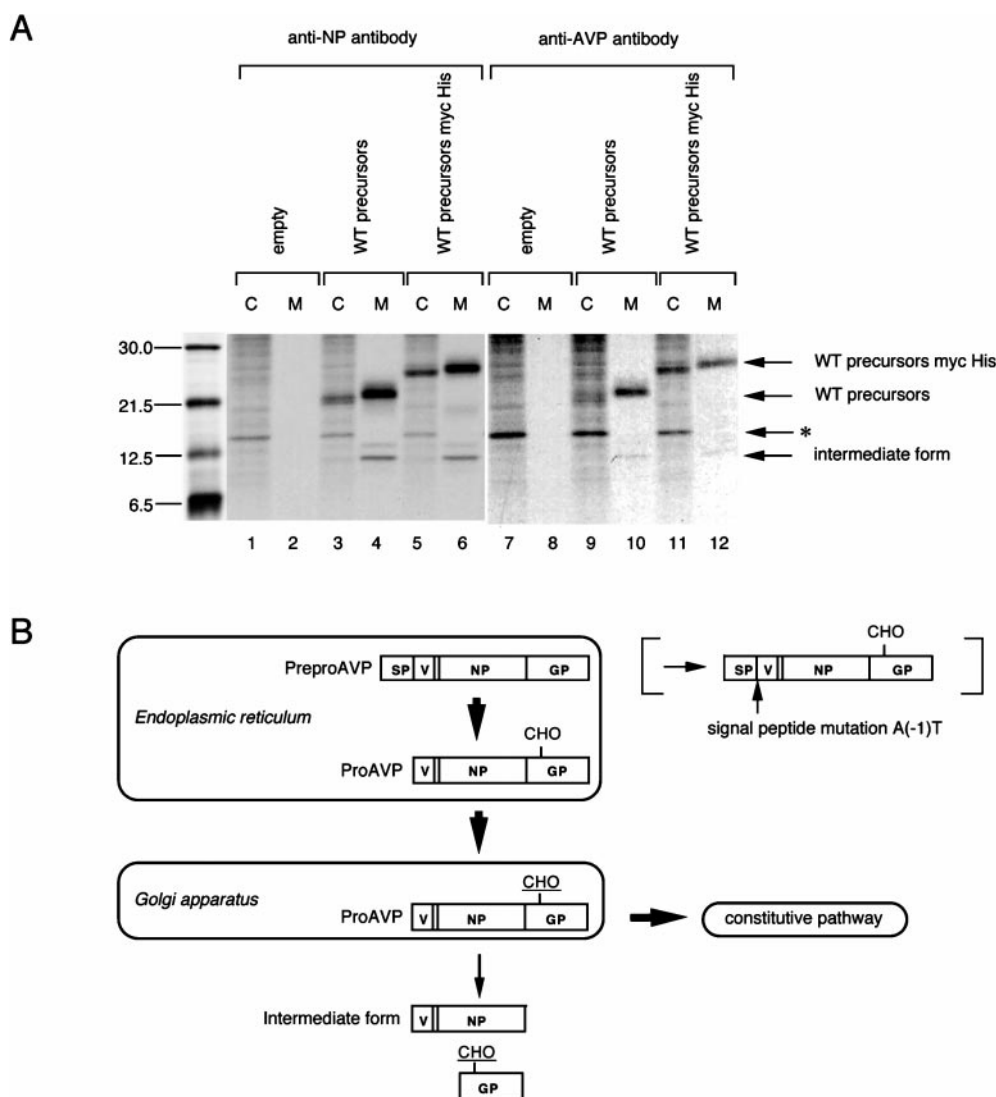


FIG. 2. Processing of WT AVP precursors. *A*, proteins produced in transiently transfected tsa 201 cells were continuously labeled with [³⁵S]methionine and cysteine. Cell extracts (*C*) and media (*M*) were subjected to immunoprecipitation using either anti-NP or anti-AVP antibodies, and the proteins were analyzed by 16.5% SDS-PAGE and autoradiography. A 14-kDa nonspecific band is denoted by an *asterisk*. Molecular mass markers are indicated to the left. Bands corresponding to WT or Myc-His-tagged precursors are indicated by *arrows*. *B*, shown is a schematic representation of post-translational processing and intracellular trafficking of AVP precursors in tsa 201 cells. Prepro-AVP is converted to pro-AVP by the removal of the signal peptide and by the addition of carbohydrate within the ER. Pro-AVP that is partially glycosylated within the ER (21 kDa) is glycosylated further within the Golgi apparatus (shown by the *underline*). Most of the terminally glycosylated pro-AVP (22 kDa) is constitutively exported into the medium. A small fraction of the glycosylated precursors undergo proteolytic processing, yielding the intermediate form, consisting of the AVP and NP domains (12 kDa). Inefficient cleavage of the A(-1)T precursor by signal peptidase results in a 23-kDa aberrant precursor that is glycosylated, but is not cleaved by signal peptidase. *SP*, signal peptide; *V*, AVP; *GP*, glycoprotein.

domains. The 12-kDa protein corresponds to the intermediate form observed in neuro2A cells (Fig. 2*B*) (23). These experiments demonstrate that the sizes of the processed AVP precursor products in this cell line and indicate that the presence of the Myc-His epitope tag does not alter the level or the efficiency of precursor processing or secretion into the medium.

Digestion of the immunoprecipitated proteins with Endo H (Fig. 3*A*) demonstrated that the WT intracellular precursors (21 and 25 kDa) (*lanes 1* and *11*) were sensitive to Endo H, yielding 17- and 21-kDa digested products (*lanes 21* and *31*). In contrast, the products in the medium (*lanes 2* and *12*) were resistant to Endo H digestion (*lanes 22* and *32*). The Endo H resistance of the secreted precursors is consistent with their increased molecular size, likely reflecting glycosylation within the Golgi apparatus. Little or no Endo H-resistant precursors were detected within cells (*lanes 21* and *31*), suggesting that AVP precursors are rapidly exported into the medium or undergo further processing once they are glycosylated within the

Golgi apparatus (Fig. 2*B*).

Post-translational Processing and Intracellular Trafficking of Mutant AVP Precursors—The expression and processing of the G57S, A(-1)T, ΔE47, and C67X mutant AVP precursors were examined in parallel with the WT precursors described above. Under conditions of continuous labeling (Fig. 3*A*), the mutant AVP precursors with and without the Myc-His tag were readily detected within cells (*lanes 1, 3, 5, 7, and 9* and *lanes 11, 13, 15, 17, and 19*). In fact, in most cases, the level of mutant precursor expression was greater than that of WT precursor expression (*lanes 1* and *11*). The migration of the G57S precursors (*lanes 3* and *13*) was indistinguishable from that of the WT precursors, whereas the A(-1)T (*lanes 5* and *15*) and ΔE47 (*lanes 7* and *17*) precursors migrated differently. The slower migration of the A(-1)T mutant likely reflects the formation of aberrant precursors that are glycosylated, but not cleaved by signal peptidase (Fig. 2*B*) (4, 23). The slightly faster migration of the ΔE47 mutant may reflect the deletion of a single amino

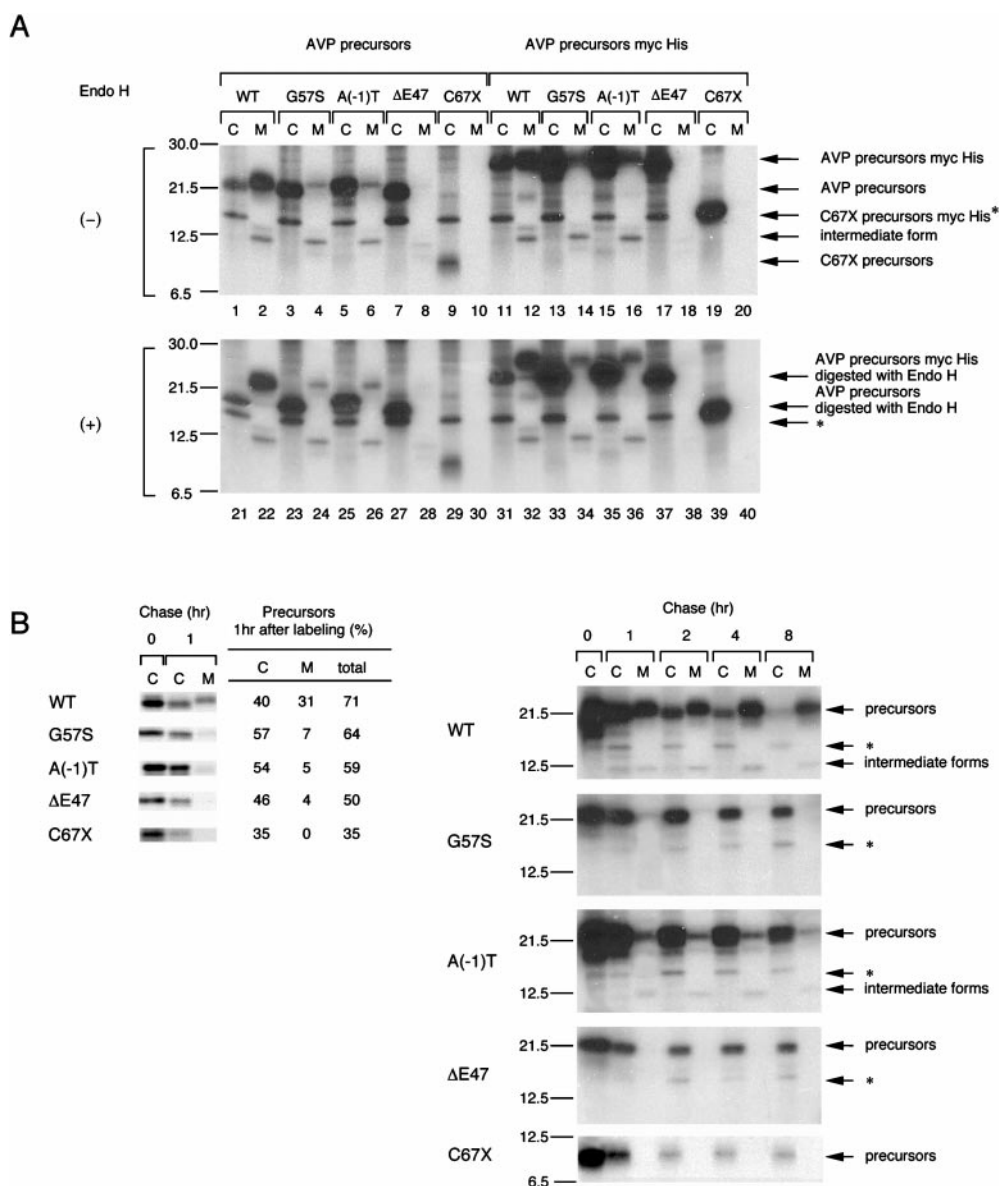


FIG. 3. Metabolic labeling of cells expressing WT or mutant AVP precursors. *A*, cells expressing WT or mutant precursors with or without the Myc-His tag were continuously labeled for 12 h. Cell extracts (C) and media (M) were subjected to immunoprecipitation using the anti-NP antibody. Immunoprecipitates were treated with or without Endo H to remove carbohydrates. Samples were separated by 16.5% SDS-PAGE followed by autoradiography. The band corresponding to the C67X precursors with the Myc-His tag (14 kDa) overlaps a nonspecific band (*). Molecular mass markers are indicated, and bands corresponding to WT or Myc-His-tagged precursors are shown by arrows. *B*, cells expressing WT or mutant precursors were labeled for 15 min and chased for the indicated times. Cell extracts and media were subjected to immunoprecipitation using the anti-NP antibody. The left panel shows data from films with exposures in the linear range. The amount of precursors in cells and the medium 1 h after the pulse labeling is expressed as a percentage of the total radiolabeled precursors present after the labeling. The right panel shows data from films with a longer exposure. The asterisks indicate a 14-kDa nonspecific band.

acid. The C67X mutant, with and without the Myc-His tag (14 and 10 kDa) (Fig. 3A, lanes 9 and 19), was also expressed well within cells. In the medium, 22- and 26-kDa precursors as well as 12-kDa intermediate forms were detected for the WT, G57S, and A(-1)T mutants (lanes 2, 4, and 6 and lanes 12, 14, and 16). The sizes of the secreted WT and A(-1)T mutant precursors in the medium were the same because their products are identical once the signal peptide is removed. The amount of the G57S and A(-1)T proteins detected in the medium was reduced compared with that of the WT protein. Little or no precursors were detectable in the medium for the ΔE47 and C67X mutants (lanes 8 and 10 and lanes 18 and 20).

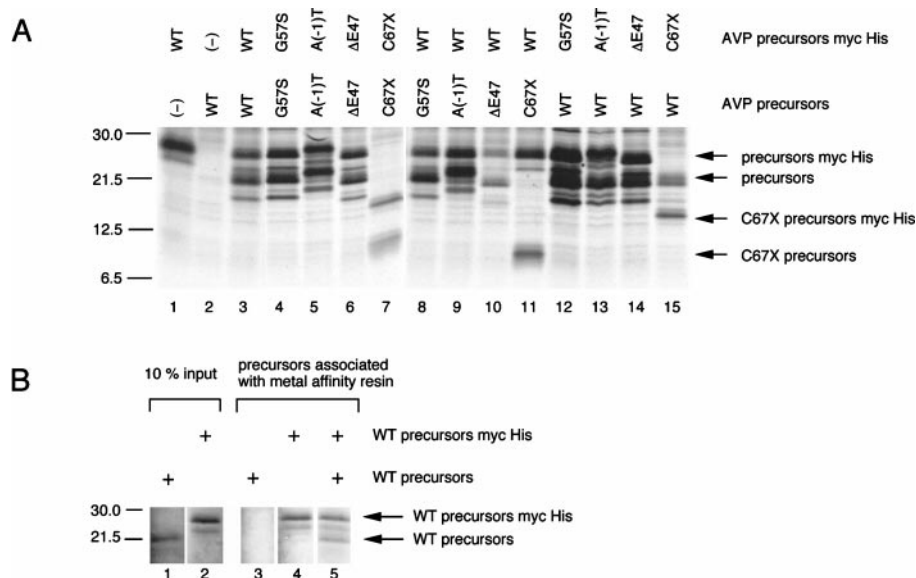
The effects of Endo H treatment were similar for the mutant and WT precursors (Fig. 3A). Digestion of intracellular G57S, A(-1)T, and ΔE47 AVP precursor proteins with and without the Myc-His tag (lanes 3, 5, and 7 and lanes 13, 15, and 17) gave

rise to 17- and 21-kDa proteins (lanes 23, 25, and 27 and lanes 33, 35, and 37). The G57S and A(-1)T precursors in the medium (lanes 4 and 6 and lanes 14 and 16) were resistant to Endo H digestion (lanes 24 and 26 and lanes 34 and 36). No Endo H-resistant precursors were detected within the cells, indicating that like the WT precursors, most of the mutant precursors are readily secreted into the medium after glycosylation within the Golgi apparatus. As expected, Endo H had no effect on the C67X mutant precursors (lanes 9 and 19 and lanes 29 and 39).

Pulse-chase analyses were performed to further evaluate the kinetics of precursor processing and secretion. AVP precursors recovered in cells and in the medium 1 h after the pulse labeling were normalized to the amount of labeled products present after labeling (Fig. 3B, left panel). The recovery of WT precursors in the medium was 31%, whereas that of the mutants ranged between 0 and 7%, indicating reduced secretion of mu-

FIG. 4. Detection of AVP precursor interactions using a metal affinity resin.

A, cells transfected with expression vectors for precursors with or without the Myc-His tag were continuously labeled with [³⁵S]methionine and cysteine. After labeling, cell extracts were incubated with the metal affinity resin. Bound proteins were separated by 16.5% SDS-PAGE followed by autoradiography. **B**, WT precursors with or without the Myc-His tag were synthesized by *in vitro* translation in the presence of microsomal membranes. The labeled precursors (5 μ l) were subjected to the interaction assay as described under "Experimental Procedures."



tant precursors. The total recovery of WT precursors in cells and the medium was 71%, whereas the recovery of the C67X mutant precursor was only 35%. In the case of other mutant precursors, the recovery was between 50 and 64%. These results suggest that intracellular degradation is involved in the inefficient secretion of mutant precursors.

Pulse-chase analyses also revealed that mutant precursors were still retained within cells 8 h after pulse labeling (Fig. 3B, right panel). By comparison, most of the WT precursors were secreted into the medium by 8 h, indicating that the mutant AVP precursors are secreted into the medium less efficiently than the WT precursors. Because precursors appear to be rapidly secreted into the medium after glycosylation (Fig. 3A), these findings suggest that the G57S, A(-1)T, and Δ E47 mutant precursors are not transported from the ER to the Golgi apparatus as effectively as the WT precursors. The levels of the C67X mutant were relatively low due to intracellular degradation (see above), but it, too, appears to be retained within the intracellular pool, consistent with previous studies in which ER retention of the C67X precursors was demonstrated using immunofluorescence staining in neuro2A cells (23). Taken together, these results show that both intracellular degradation and retention are responsible for the reduced secretion of mutant precursors.

Physical Interaction of AVP Precursors—AVP precursors were previously shown to interact with each other *in vitro* using synthetic peptides and immobilized NP (25). We used a protein "pull-down" assay to assess interactions among the precursor proteins. Cells were treated with BFA, which blocks protein transport from the ER to the Golgi apparatus, to allow a similar degree of retention of both mutant and WT AVP precursors. Treatment of cells with BFA completely eliminated the release of precursors and intermediate forms into the medium, resulting in a comparable degree of WT and mutant precursor expression (data not shown). Cells expressing precursors with and without the Myc-His tag were labeled in the presence of BFA prior to lysis. Cell extracts were incubated with metal affinity resin to bind AVP precursors containing the Myc-His tag to the resin. After extensive washing, bound proteins were separated on 16.5% SDS-polyacrylamide gels followed by autoradiography (Fig. 4A). AVP precursors with the Myc-His tag were retained by the metal affinity resin (lane 1), but those without the Myc-His tag were not retained (lane 2), demonstrating a specific interaction of the His₆-tagged precursors with the resin.

WT and mutant precursors with the Myc-His tag interacted with their respective precursors without the tag (Fig. 4A, lanes 3–7), as reflected by the fact that the precursors without the Myc-His tag were also retained by the affinity column. These results suggest that WT and mutant precursors form homodimers. WT precursors with the Myc-His tag also interacted with the G57S, A(-1)T, Δ E47, and C67X mutant precursors (lanes 8–11). And in the reverse format, the G57S, A(-1)T, Δ E47, and C67X mutant precursors with the Myc-His tag interacted with the WT precursors (lanes 12–15). These results indicate that the WT and mutant precursors form both homo- and heterodimers.

Precursor proteins were also labeled during *in vitro* translation to provide an estimate of the fraction of input proteins that interact with the metal affinity resin in this assay (Fig. 4B). WT precursors with and without the Myc-His tag were translated *in vitro* in the presence of microsomal membranes to produce prohormones (4). WT precursors with the Myc-His tag (25 kDa) (lane 2) interacted with metal affinity resin (lane 4). WT precursors (21 kDa) (lane 1) without the tag did not interact with the resin (lane 3), but were retained in the presence of WT precursors with the Myc-His tag (lane 5). In comparison with the input proteins (lanes 2 and 4), ~8% of the WT precursors with the Myc-His tag were bound, which is similar to the interactions of previously characterized protein dimers in this type of assay (30). Approximately 7% of the total input of WT precursors without the tag was associated with WT precursors with the Myc-His tag (lanes 1 and 5), suggesting that the majority of WT precursors without the tag interact with WT precursors with the epitope tag.

Homodimerization of WT and Mutant AVP Precursors—Cross-linking studies were used to further assess the formation of AVP precursor homodimers within the cellular environment. WT or mutant precursors with the HA tag were expressed, and the cells were subjected to an *in vivo* cross-linking reaction with DSS prior to lysis. After Western blot transfer, membranes were probed with an anti-HA antibody (Fig. 5). The monomeric form of the WT, G57S, A(-1)T, and Δ E47 precursors was 23 kDa, whereas the C67X monomer was 12 kDa. In the absence of DSS treatment, homodimerization of the G57S and Δ E47 precursors (46 kDa) was detected (lanes 3 and 7), but little or no homodimerization was seen with the WT, A(-1)T, and C67X (24 kDa) precursors (lanes 1, 5, and 9). After treatment with DSS, all of the WT and mutant precursors formed homodimers (lanes 2, 4, 6, 8, and 10). The ratio of dimer to

FIG. 5. Evidence for homodimer formation of WT and mutant precursors using protein cross-linking. Cells expressing WT or mutant precursors with the HA tag were incubated in the presence or absence of 1 mM DSS for 30 min. After the cross-linking reaction, whole cell extracts were prepared and loaded onto 15% SDS-polyacrylamide gels. After Western blot transfer, polyvinylidene difluoride membranes were probed with the anti-HA antibody. The asterisk indicates a nonspecific band.

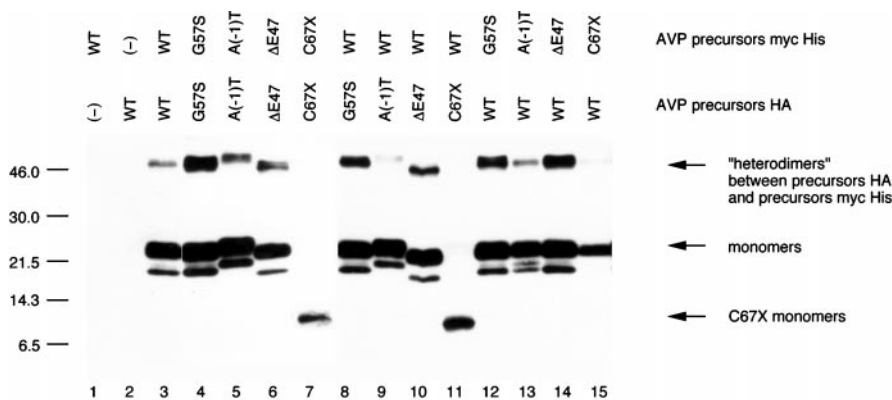
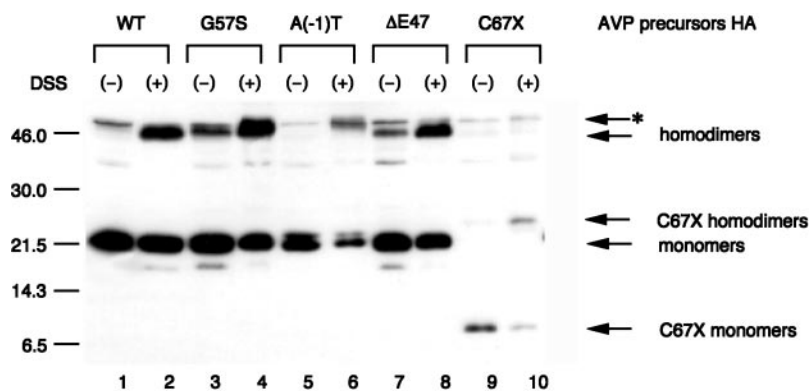


FIG. 6. Evidence for heterodimer formation between WT and mutant AVP precursors. Cells expressing precursors containing the Myc-His tag and those containing the HA tag were subjected to the cross-linking reaction *in vivo*. After the reaction, cell extracts were prepared and incubated with the metal affinity resin. Bound proteins were eluted from the resin and separated by 15% SDS-PAGE. After Western blot transfer, membranes were probed with the anti-HA antibody.

monomer for the C67X mutant was greater than that for the WT, G57S, A(-1)T, and ΔE47 precursors.

Heterodimerization of WT and Mutant AVP Precursors—Cells coexpressing WT and mutant precursors with the HA tag and the Myc-His tag were subjected to the cross-linking reaction with DSS prior to lysis. Cell extracts were prepared and incubated with the metal affinity resin to isolate Myc-His-tagged complexes. After washing, bound proteins were subjected to Western blot transfer, and the membranes were probed with the anti-HA antibody (Fig. 6). As a control, WT precursors with the Myc-His tag were not recognized by the anti-HA antibody (*lane 1*). WT precursors with the HA tag were not detected in the absence of precursors with the Myc-His tag (*lane 2*), indicating that the precursors with the HA tag were not retained by the affinity resin. However, WT precursors with the HA tag were detected when coexpressed with WT precursors containing the Myc-His tag (*lane 3*). The detection of 48-kDa proteins by the anti-HA antibody indicates the formation of mixed complexes consisting of WT precursors with the Myc-His tag (25 kDa) and those with the HA tag (23 kDa) (*lane 3*). Similarly, homodimerization of G57S, A(-1)T, and ΔE47 precursors was demonstrated by the detection of complexes consisting of the Myc-His- and HA-tagged precursors (*lanes 4–6*). Little or no homodimerization was seen with the C67X precursors (*lane 7*).

WT precursors with the Myc-His tag also formed heterodimers with the G57S, A(-1)T, and ΔE47 precursors (Fig. 6, *lanes 8–10*). Similarly, the G57S, A(-1)T, and ΔE47 precursors heterodimerized with the WT precursors (*lanes 12–14*). Heterodimerization between the WT and the G57S and ΔE47 mutant precursors was prominent, whereas heterodimer formation between the WT and A(-1)T precursors was relatively weak. Little or no heterodimerization was detected between the WT and C67X precursors (*lanes 11 and 15*). Most of the monomeric forms of the HA-tagged precursors are likely derived from a physical interaction with precursors with the Myc-His

tag during the incubation with metal affinity resin. Thus, the physical interaction between monomeric form of precursors detected in this experiment is similar to that detected in the precursor interaction assay (Fig. 4A).

Dominant-negative Effect of Mutant AVP Precursors—Because mutant precursors are not efficiently exported into the medium, it is possible that they might also alter the transport and processing of the WT AVP precursors. WT or mutant precursors with the Myc-His tag were coexpressed in cells with WT precursors that did not contain an epitope tag. After continuous labeling, cell extracts and medium were immunoprecipitated using the anti-NP antibody (Fig. 7). Consistent with previous findings (Fig. 3A), the amount of secreted G57S, A(-1)T, ΔE47, and C67X mutant precursors with the Myc-His tag was reduced compared with that of the WT precursors with the Myc-His tag, suggesting retention of mutant precursors (Fig. 7A). The ratios of secreted to intracellular precursors were 0.23, 0.37, 0.14, and 0.06 for the G57S, A(-1)T, ΔE47, and C67X precursors, respectively. By comparison, the ratio for the WT precursors was 1.38 (Fig. 7B). When WT precursors with the Myc-His tag were coexpressed (Fig. 7C), WT precursors without an epitope tag were effectively exported into the medium (ratio = 1.30). However, when coexpressed with the G57S, A(-1)T, ΔE47, or C67X mutant precursor containing the Myc-His tag, more WT precursors were detected within cells, and secretion of the WT precursors was decreased, resulting in ratios of 0.40, 0.73, 0.48, and 0.85, respectively. The retention of intracellular WT precursors was more prominent with coexpression of the G57S, A(-1)T, and ΔE47 mutants. When the C67X precursors with the Myc-His tag were coexpressed, the amount of intracellular WT precursors and secreted precursors was decreased. Taking into account the increased degradation of the C67X precursors (Fig. 3B), it is possible that WT precursors retained within the ER through heterodimer formation with the C67X precursors were degraded along with the mutant precursors.

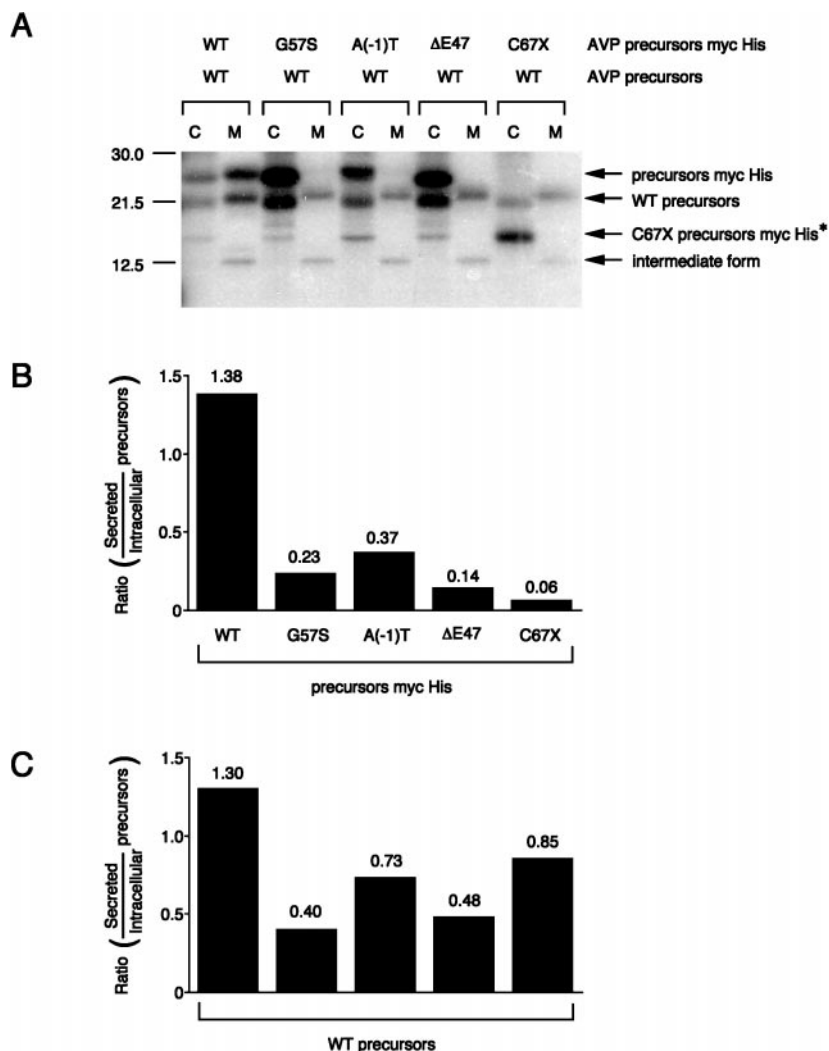


FIG. 7. Mutant precursors impair the transport and processing of WT AVP precursors. *A*, cells expressing WT or mutant precursors containing the Myc-His tag and WT precursors without the epitope tag were continuously labeled. Cell extracts (*C*) and media (*M*) were immunoprecipitated using anti-NP antibodies followed by 16.5% SDS-PAGE and autoradiography. The band corresponding to the C67X precursors with the Myc-His tag (14 kDa) overlaps a nonspecific band (*). *B*, the ratio of secreted precursors containing the Myc-His tag to intracellular precursors was determined using densitometric analyses. *C*, the ratio of secreted to intracellular WT precursors is shown. The S.E. for different samples in *B* and *C* ranged from 0.01 to 0.04.

DISCUSSION

The structure-function relationship of the NP molecules has been intensively studied (for review, see Ref. 31). NP consists of two highly homologous domains that arose from a partial gene duplication (Fig. 4*B*) (32). These structural features underlie the propensity of NP molecules to self-associate (33) and form larger aggregates under acidic pH (34). The fully processed hormone AVP binds to NP (35, 36) and induces a greater degree of self-association (37). NMR analysis of crystallized NP molecules revealed the residues involved in NP binding to AVP and indicated that the interface for the monomer-monomer interaction (codons 32–37 and 77–82) forms a β -sheet structure (38). Using a semisynthetic precursor and immobilized NP, AVP precursors have been shown to exhibit characteristics similar to those of NP molecules (25, 39). The precursors self-associate through the NP domains, and the intramolecular interaction between the AVP and NP domains enhances self-association, suggesting that higher order aggregates of precursors may also be formed. These previous *in vitro* studies suggested the possibility that mutant AVP precursors might interact with WT precursors and affect their function *in vivo*.

To study the interactions among different AVP precursors *in vivo*, it is necessary to be able to distinguish them from one another. For this reason, we attached two different epitopes to the precursors. The epitopes were added immediately after the last codon of the WT and mutant precursors to minimize the potential effects of epitope tagging on precursor function (Fig. 1*B*). In addition to its other features, the Myc-His epitope is

large enough that epitope-tagged precursors can be distinguished from non-epitope-tagged precursors because of differences in molecular mass (~ 3 kDa greater). The observed migration of precursors without the tag was 21 kDa *versus* 25 kDa with the Myc-His tag. The slightly slower migration of the Myc-His-tagged precursors may be caused by the presence of the unusual stretch of polyhistidine codons. Since post-translational processing and intracellular trafficking of precursors with the Myc-His tag were similar to those of precursors without the epitope tag (Figs. 2*A* and 3*A*), the addition of epitope to the carboxyl-terminal end of the AVP precursors does not appear to affect the processing or transport of the precursors. The Myc-His tag also allows selective isolation of AVP precursors using the metal affinity resin. Precursors with the Myc-His tag were shown to interact specifically with the resin, whereas precursors without the tag and those with the HA tag did not bind to the resin (Figs. 4*A* and 6). The other epitope, HA, was added to distinguish precursors using an anti-HA antibody. Precursors without the HA epitope tag and those with the Myc-His tag were not recognized by the anti-HA antibody (data not shown). Taken together, these two strategies for epitope tagging of the AVP precursors provide useful tools for examining their interactions with each other and potentially other cellular proteins.

The precursor interaction assay revealed an effective physical association of AVP precursors (Fig. 4*A*). In this assay, dimers formed during the incubation with the metal affinity resin as well as those formed within the ER were detected.

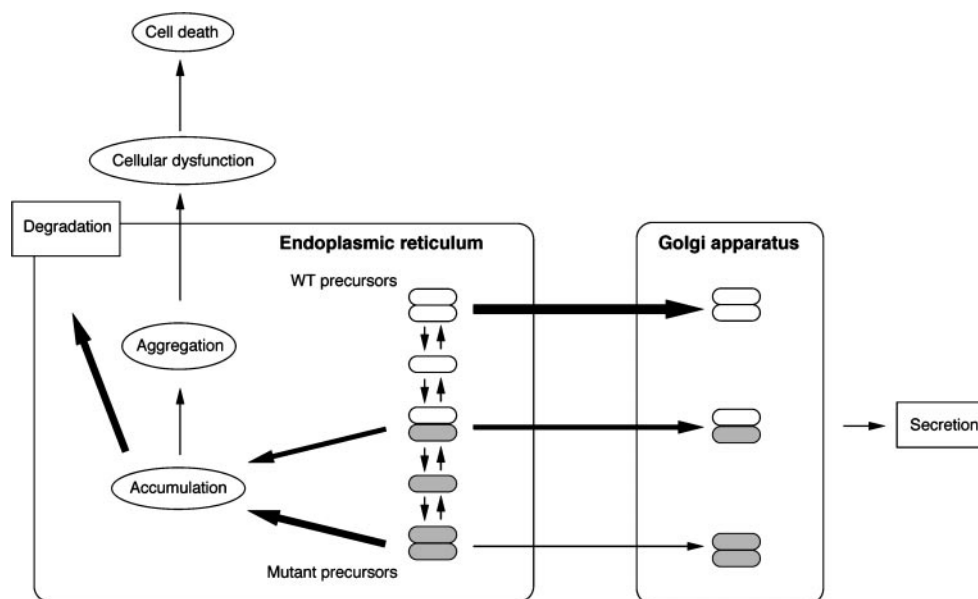


FIG. 8. **Proposed model for the molecular basis of FNDI.** Functional and physical interactions occur between WT and mutant precursors that are retained within the ER. The mutant precursors impair the transport and processing of the WT precursors. The accumulation and aggregation of mutant-mutant and mutant-WT precursors lead to cellular toxicity (23). Thus, the pathogenesis of FNDI may involve direct cellular toxicity of the mutant AVP precursors as well as a dominant-negative effect of the mutant precursors on the transport and processing of the WT gene product.

Thus, evidence of a physical interaction in this assay does not necessarily imply that dimerization occurred within the ER. For this reason, we also used an *in vivo* cross-linking reaction that was performed prior to cell lysis to examine intracellular dimerization of precursors. The use of a non-cleavable cross-linker prevents the dissociation of dimers after cell lysis. For the detection of homodimers, cells were incubated in the absence or presence of cross-linker prior to lysis (Fig. 5). When treated with the cross-linker, apparently all of the WT and mutant precursors formed homodimers. In the absence of the cross-linker, little or no homodimers were detected for the WT, A(-1)T, and C67X precursors. In contrast, the G57S and Δ E47 precursors readily formed homodimers. It is notable that the G57S and Δ E47 homodimers were detected by reducing SDS-PAGE, suggesting that these homodimers are tightly bound. In the subsequent experiments in which the *in vivo* cross-linking and affinity reactions were combined (Fig. 6), homodimerization of the G57S and Δ E47 precursors was confirmed to be relatively strong in comparison with the other precursors (G57S > Δ E47 = A(-1)T > WT >> C67X). In the same experiment (Fig. 6), heterodimerization between WT and mutant precursors was analyzed, and the G57S and Δ E47 mutant precursors were also found to form heterodimers with WT precursors more effectively than the A(-1)T and C67X precursors. Most of the A(-1)T precursors detected within the cells are likely to be aberrant precursors anchored to the ER membranes via the signal peptide (Fig. 2B). This may explain the reduced detection of homodimers as well as a smaller amount of heterodimers with WT precursors (Figs. 5 and 6). The C67X precursors lack 5 out of 14 cysteine residues within the NP domain, but still contain a single β -sheet structure, which may be involved in the monomer-monomer interaction. Some degree of C67X homodimerization was detected in some paradigms (Fig. 5), but not in others (Fig. 6). In addition, heterodimerization with WT precursors was not detectable (Fig. 6). The extent of dimerization appears to differ in the two different assays. However, the intracellular cross-linking assay using the metal affinity resin (Fig. 6) is probably less sensitive than the other intracellular cross-linking assay (Fig. 5). Based on data using the precursor interaction assay (Fig. 4), it is likely that the

C67X precursors heterodimerize, to some extent, with WT precursors. The lack of the second β -sheet structure in the C67X mutant may account for reduced homo- and heterodimer formation in comparison with WT or other mutant precursors. In summary, these data show that WT and mutant precursors form homodimers and that mutant precursors can heterodimerize with WT precursors within the ER.

Coexpression of WT and mutant precursors revealed impaired transport of WT precursors from the ER to the Golgi apparatus in the presence of the mutant precursors (Fig. 7). This effect was particularly prominent when the G57S, A(-1)T, and Δ E47 precursors were coexpressed with the WT protein. The C67X precursors had less effect on the transport of WT precursors. We propose that this dominant-negative effect is mediated through heterodimer formation of WT precursors with mutant precursors that are retained within the ER. The observation that the C67X precursors exhibit less pronounced dominant-negative activity correlates with the relative lack of heterodimerization between the WT and C67X mutant precursors (Fig. 6).

We have previously shown that mutant AVP precursors may induce neuronal cell death as a result of their accumulation within the ER (23). Although much of the mutant precursor protein that is accumulated within the ER may be degraded, part may form aggregates over time, eventually perturbing cellular function and leading to cell death (Fig. 8). In this study, we provide evidence that mutant AVP precursors can form heterodimers with WT precursors and impair the production of AVP from the normal allele. This dominant-negative effect of mutant precursors on the transport of WT precursors from the ER to the Golgi apparatus may account, in part, for the autosomal dominant mode of inheritance, but it cannot explain the delayed onset of the disease. It is therefore more likely that the cytotoxicity of the mutant precursors is the primary cause of the disease. The formation of heterodimers between WT and mutant precursors may also contribute to the cytotoxicity. It is notable that among the many naturally occurring mutations in the AVP gene, there are no missense mutations within the β -sheet structures that are involved in the monomer-monomer interaction. Also, all nonsense mutations reported to date are

located within the carboxyl-terminal region of the NP domain (C61X, C67X, C79X, E81X, P83X, and E87X). The fact that the C67X precursors are functional in terms of dimer formation makes it less likely that mispaired disulfide bonds are formed in the truncated precursors. Rather, the truncated precursors may retain the first β -sheet structure. In this study, each of the four representative mutant precursors, G57S, A(-1)T, Δ E47, and C67X, formed dimers with WT precursors. It is likely, but will require further study, that all the mutant precursors found in FNDI may form heterodimers with WT precursors. The cytotoxicity that was observed in a previous study (23) varied among the different mutants (C67X > A(-1)T > G57S > Δ E47). On the other hand, the rank order of heterodimer formation determined in this study was the inverse (Δ E47 = G57S > A(-1)T \gg C67X). For example, the Δ E47 mutant, which showed the least cytotoxic effect among the mutants, interacted with WT precursors the best, whereas the C67X mutant, which exhibited the greatest degree of cytotoxicity, formed heterodimers with WT precursors least effectively. It is likely that both dominant-negative activity and cytotoxicity are involved in the pathogenesis of FNDI. Because mutant-WT dimers may also be cytotoxic, these mechanisms are not mutually exclusive.

REFERENCES

- Baylis, P. H. (1995) in *Endocrinology* (DeGroot, L. J., ed), 3rd Ed., pp. 406–420, W. B. Saunders Co., Philadelphia
- Ito, M., Mori, Y., Oiso, Y., and Saito, H. (1991) *J. Clin. Invest.* **87**, 725–728
- Bahnsen, U., Oosting, P., Swaab, D. F., Nahke, P., Richter, D., and Schmale, H. (1992) *EMBO J.* **11**, 19–23
- Ito, M., Oiso, Y., Murase, T., Kondo, K., Saito, H., Chinzei, T., Racchi, M., and Lively, M. O. (1993) *J. Clin. Invest.* **91**, 2565–2571
- Yuasa, H., Ito, M., Nagasaki, H., Oiso, Y., Miyamoto, S., Sasaki, N., and Saito, H. (1993) *J. Clin. Endocrinol. Metab.* **77**, 600–604
- Krishnamani, M. R., Phillips, J. A. I., and Copeland, K. C. (1993) *J. Clin. Endocrinol. Metab.* **77**, 596–598
- McLeod, J. F., Kovacs, L., Gaskill, M. B., Rittig, S., Bradley, G. S., and Robertson, G. L. (1993) *J. Clin. Endocrinol. Metab.* **77**, 599A–599G
- Repaske, D. R., and Browning, J. E. (1994) *J. Clin. Endocrinol. Metab.* **79**, 421–427
- Nagasaki, H., Ito, M., Yuasa, H., Saito, H., Fukase, M., Hamada, K., Ishikawa, E., Katakami, H., and Oiso, Y. (1995) *J. Clin. Endocrinol. Metab.* **80**, 1352–1356
- Rauch, F., Lenzner, C., Nurnberg, P., Frommel, C., and Vetter, U. (1996) *Clin. Endocrinol.* **44**, 45–51
- Rittig, S., Robertson, G. L., Siggaard, C., Kovacs, L., Gregerse, N., Nyborg, J., and Pedersen, E. B. (1996) *Am. J. Hum. Genet.* **58**, 107–117
- Rutishauser, J., Boni-Schnetzler, M., Boni, J., Wichmann, W., Huisman, T., Vallotton, M. B., and Froesch, E. R. (1996) *J. Clin. Endocrinol. Metab.* **81**, 192–198
- Ueta, Y., Taniguchi, S., Yoshida, A., Murakami, I., Mitani, Y., Hisatome, I., Manabe, I., Sato, R., Tsuboi, M., Ohtahara, A., Nanba, E., and Shigemasa, C. (1996) *J. Clin. Endocrinol. Metab.* **81**, 1787–1790
- Heppner, C., Kotzka, J., Bullmann, C., Krone, W., and Muller-Wieland, D. (1998) *J. Clin. Endocrinol. Metab.* **83**, 693–696
- Calvo, B., Bilbao, J. R., Urrutia, I., Eizaguirre, J., Gaztambide, S., and Castano, L. (1998) *J. Clin. Endocrinol. Metab.* **83**, 995–997
- Sausville, E., Carney, D., and Batten, J. (1985) *J. Biol. Chem.* **260**, 10236–10241
- Brownstein, M. J., Russel, J. T., and Gainer, H. (1980) *Science* **207**, 373–378
- Hansen, L. K., Rittig, S., and Robertson, G. L. (1997) *Trends Endocrinol. Metab.* **8**, 363–372
- Braverman, L. E., Mancini, J. P., and McGoldrick, D. M. (1965) *Ann. Intern. Med.* **63**, 503–508
- Green, J. R., Buchan, G. C., Alvord, E. C., and Swanson, A. G. (1967) *Brain* **90**, 707–714
- Nagai, I., Li, C. H., Hsieh, S. M., Kizaki, T., and Urano, Y. (1984) *Acta Endocrinol.* **105**, 318–323
- Bergeron, C., Kovacs, K., Ezrin, C., and Mizzen, C. (1991) *Acta Neuropathol.* **81**, 345–348
- Ito, M., Jameson, J. L., and Ito, M. (1997) *J. Clin. Invest.* **99**, 1897–1905
- Herskowitz, I. (1987) *Nature* **329**, 219–222
- Kanmera, T., and Chaiken, I. M. (1985) *J. Biol. Chem.* **260**, 8474–8482
- Sanger, F., Nicklen, S., and Coulson, A. R. (1977) *Proc. Natl. Acad. Sci. U. S. A.* **74**, 5463–5467
- Margolskee, R. F., McHendry-Rinde, B., and Horn, R. (1993) *BioTechniques* **15**, 906–911
- Graham, F. L., and van der Eb, A. J. (1973) *Virology* **52**, 456–487
- Misumi, Y., Misumi, Y., Miki, K., Takatsuki, A., Tamura, G., and Ikehara, Y. (1986) *J. Biol. Chem.* **261**, 11398–11403
- Ito, M., Yu, R., and Jameson, J. L. (1997) *Mol. Cell. Biol.* **17**, 1476–1483
- de Bree, F. M., and Burbach, J. P. (1998) *Cell. Mol. Neurobiol.* **18**, 173–191
- Breslow, E., and Burman, S. (1990) *Adv. Enzymol. Relat. Areas Mol. Biol.* **63**, 1–67
- Angal, S., and Chaiken, I. M. (1982) *Biochemistry* **21**, 1574–1580
- Breslow, E., Aanning, H. L., Abrash, L., and Schmir, M. (1971) *J. Biol. Chem.* **246**, 5179–5188
- Breslow, E., and Walter, R. (1972) *Mol. Pharmacol.* **8**, 75–81
- Breslow, E., Weis, J., and Menendez-Botet, C. J. (1973) *Biochemistry* **12**, 4644–4653
- Nicolas, P., Wolff, J., Camier, M., Di Bello, C., and Cohen, P. (1978) *J. Biol. Chem.* **253**, 2633–2639
- Chen, L. Q., Rose, J. P., Breslow, E., Yang, D., Chang, W. R., Furey, W. F. J., Sax, M., and Wang, B. C. (1991) *Proc. Natl. Acad. Sci. U. S. A.* **88**, 4240–4244
- Ando, S., McPhie, P., and Chaiken, I. M. (1987) *J. Biol. Chem.* **262**, 12962–12969